Kovove Mater. 52 2014 231–236
DOI: 10.4149/km_2014_4_231

Diffusion kinetics of different boronizing processes on martensitic stainless steel AISI 420

P. Juijerm*

Materials Innovation Center and Department of Materials Engineering – Metals Research Group, Faculty of Engineering, Kasetsart University, 50 Ngamwongwan Rd., Ladyao, Jatujak, Bangkok 10900, Thailand

Received 5 December 2013, received in revised form 8 February 2014, accepted 3 March 2014

Abstract

Martensitic stainless steels are much more considered using in many applications relating high loading and wear. A boride layer on martensitic stainless steel is generally accepted against wear and oxidation occurred during services. Boronizing processes, salt bath and powder pack, were performed on a martensitic stainless steel AISI 420 at a temperature range of 1123–1223 K with boronizing time up to 9 h. Boride layer thicknesses were measured using an optical microscope with an image analyzer program. An X-ray diffraction (XRD) and a scanning electron microscope with energy dispersive X-ray spectroscopy (SEM-EDS) were performed to characterize the boride layers. Kinetics of boronizing processes was analyzed using diffusion and Arrhenius equations. Activation energies and empirical data of the boronizing processes will be determined. It was found that the thicknesses of the boride layers increase with increasing boronizing temperature and time taking into account diffusion theory. Activation energies of 233.5 and 185.2 kJ mol^{-1} were determined and discussed for martensitic stainless steel AISI 420 boride in a salt bath and powder pack, respectively. Finally, empirical relationships of boride thickness as a function of boronizing temperature and time are presented.

K e y w o r d s: thermochemical surface treatment, boronizing process, stainless steel, diffusion, kinetics

1. Introduction

At present, surface treatments are playing important role to improve lifetime and performance of many components involved with fatigue, wear or oxidation. Boronizing process is one of well-known thermochemical surface treatments which can be applied to various metallic materials, both ferrous and nonferrous metals. Wear resistance of metallic materials subjected to tribological applications will be significantly improved by protection of hard and low-friction-coefficient boride layers [1, 2]. Recently, martensitic stainless steels are much more considered using in many applications relating high loading and wear. A boride layer on steels is generally accepted against wear [3–5], corrosion [6–8] and oxidation [8–10] occurred during services. In the manufacturing process, boronizing temperature and time are very important factors to produce a required boride layer thickness. The boride layer thickness as a function of boronizing temperature and time is crucial to decrease trails and errors in the manufacturing process. Accordingly, operating cost and time can be saved. An empirical function of the boride layer thickness in terms of boronizing temperature and time can be constructed using the diffusion and kinetics theories. However, information about borided martensitic stainless steel AISI 420 is limited and not well established. Therefore, in this study, boronizing processes both using a salt bath and powder pack on martensitic stainless steel AISI 420 will be addressed. Diffusion and kinetics theories will be used to analyze experimental results. Activation energies and empirical data of the boronizing processes will be determined. Consequently, empirical functions of boride layer thickness in terms of boronizing temperature and time will be presented.

*Corresponding author: fax: +662 955 1811; e-mail address: juijerm@gmail.com

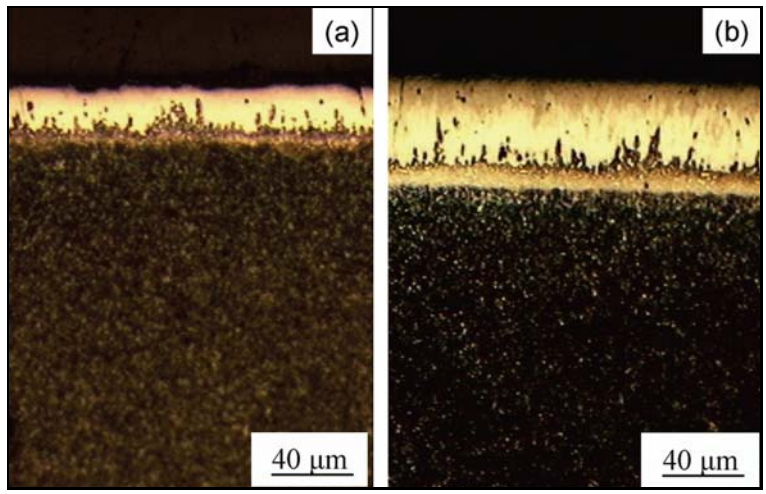

Fig. 1. Microstructures of boride layers on the martensitic stainless steel AISI 420 using (a) salt bath and (b) powder pack at a boronizing temperature of 1173 K for about 4 h.

Finally, simulated boride layer thickness as a function of boronizing temperature and time will be practically plotted and shown in a diagram for industrial usage.

2. Materials and experimental procedures

The martensitic stainless steel AISI 420 was delivered as hardened and tempered bars with a diameter of 12.5 mm. The chemical composition of this alloy is 0.3 % C, 0.25 % Si, 0.43 % Mn, 0.018 % P, 0.028 % S, 0.32 % Ni, 12.15 % Cr and Fe balance (all values in wt.%). Cylindrical specimens with a diameter of 12.5 mm and a height of 20 mm were prepared from bars of the martensitic stainless steel AISI 420. All samples were ground with 600 grit SiC paper to clean the surface. The packed boronizing process was performed using the commercial boronizing agent named Ekabor-I from BorTec GmbH, Germany. The boronizing process in a salt bath was carried out in molten borax ($Na_2B_4O_7$) added 15 wt.% ferrosilicon (Fe-Si) as an activator. All boronizing processes were operated in a temperature range of 1123–1223 K. Boronizing times up to 9 h were investigated. Microstructures and types of the existing layers were characterized using an optical microscope, SEM-EDS and XRD with Cu Kα radiation source. The thicknesses were measured using the optical microscope with an image analyzer program. Diffusion kinetics of the boronizing processes was analyzed using diffusion and Arrhenius equations.

3. Results and discussion

After boronizing treatments using molten borax with Fe-Si 15 wt.% and powder pack at the boronizing temperature range of 1123–1223 K, there are boride layers on the surfaces of the martensitic stainless steel AISI 420. Figures 1a,b show examples of boride layers on martensitic stainless steel AISI 420 using a salt bath and powder pack, respectively, at boronizing temperature of 1173 K for about 4 h. Boride layer thickness of using a salt bath is less than that of using powder packed boronizing. It should be contributed to unequal amount of free boron atoms in different processes. That means that the boronizing process using molten borax with Fe-Si 15 wt.% provides lower free boron atoms as compared to the other one using commercial powder pack. XRD phase analysis was performed to characterize the boride layers as shown in Fig. 2. Single phase, Fe_2B was detected on the martensitic stainless steel AISI 420 borided using a salt bath, whereas double phases, FeB

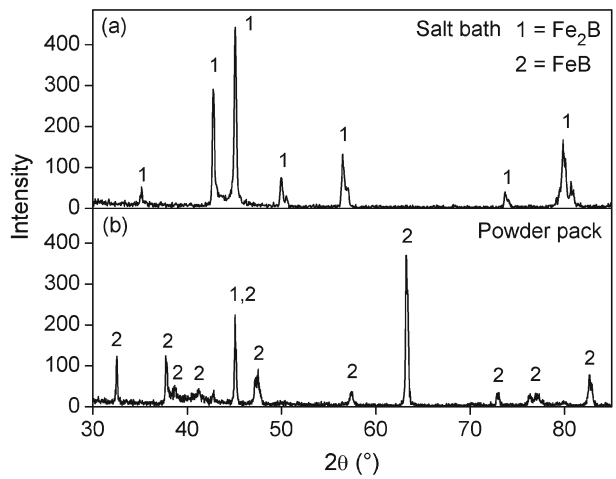

Fig. 2. XRD patterns of the martensitic stainless steel AISI 420 specimens boronized using (a) salt bath and (b) powder pack at boronizing temperatures of 1173 K for about 4 h.

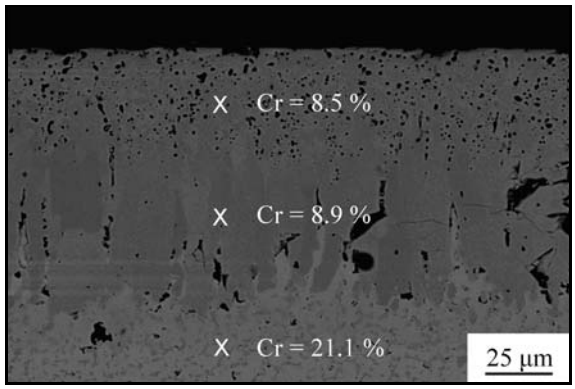

Fig. 3. SEM microstructure with EDS analysis of boride layer after packed boronizing at a temperature of 1223 K for about 4 h.

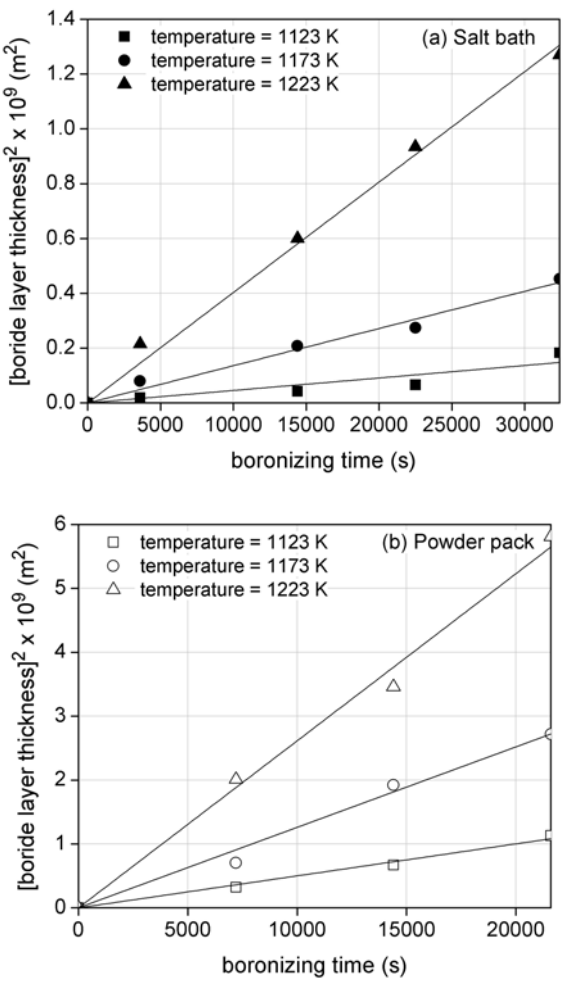

Fig. 4. Square of the boride layer thickness versus boronizing time of the martensitic stainless steel AISI 420 boronized using (a) salt bath and (b) powder pack.

and Fe_2B, were seen when powder pack was used. It is due to the fact that the double phases of boride layers will be dominated, if the concentration of free boron atoms, boronizing temperature or boronizing time increase. Moreover, the boride layer thickness and type depend strongly on alloying elements of metallic materials due to they obstruct the diffusion of boron atoms into a substrate [1, 2]. Consequently, lower thicknesses, double phases and relatively smooth and more compact morphology are the characteristics of boride layers formed on high alloy steels [11–15]. A SEM-EDS was performed to analyze the concentration of chromium in the boride layer and the transition zone as illustrated in Fig. 3, which shows the microstructure of the boride layer after boronizing process using powder pack at a boronizing temperature of 1173 K for about 4 h. Chromium contents of 8.5 and 8.9 wt.% were detected at the boride layer FeB and Fe_2B, respectively. However, in this study, the chromium boride phase was not found by XRD investigations. It is possibly due to a relative low intensity and a low volume fraction of the chromium boride phases. Normally, the chromium element has a very low solubility in the boride layer, then almost chromium atoms were pressed into the substrate during forming of the boride layer. Consequently, chromium content of 21.1 wt.% was observed in the transition zones beneath the boride layer, whereas the chromium content of the substrate was about 12 wt.%. The boride layer thickness usually increases, as the boronizing temperature rises and the treatment time becomes longer taking into account a diffusion law [1, 2, 16–19]. The squared thickness of boride layer as a function of time can be described in Eq. (1) as follows:

$$d^2 = Kt, \tag{1}$$

where d is the depth of boride layer (m), t is process time (s), K is the growth rate constant depending on the boronizing temperature and can be determined by a slope of a straight line in a diagram of d^2 as a function of boronizing time at a given boronizing temperature as shown in Figs. 4a,b for boronizing in molten borax and powder pack, respectively. The relationship between the growth rate constant, K and temperature can be expressed by the Arrhenius equation in Eq. (2) as follows:

$$K = K_0 \exp\left(-Q/RT\right), \tag{2}$$

where K_0 is a constant, Q is an activation energy (J mol^{-1}), T is an absolute temperature (K) and R is the gas constant (J mol^{-1} K^{-1}). The plot of the natural logarithm of the growth rate constant ($\ln K$) versus the reciprocal boronizing temperature reveals a linear relationship. Therefore, activation energy and empirical data, K_0, of the process can be determined by the slope and y-axis interception of this diagram, respectively, as shown in Fig. 5. The determined activ-

Table 1. Summarized boriding parameters with empirical equation including R^2 and mean absolute percentage error (MAPE)

Boronizing	Q (kJ mol^{-1})	K_0 (m^2 s^{-1})	Empirical equation d (μm), t (s), T (K)	R^2	MAPE (%)
Salt bath	233.5	3.51×10^{-4}	$d = 1.87 \times 10^4 \sqrt{t \exp\left(-\frac{28085.3}{T}\right)}$	0.972	10.9
Powder pack	185.2	2.18×10^{-5}	$d = 4.67 \times 10^3 \sqrt{t \exp\left(-\frac{22271.9}{T}\right)}$	0.988	4.26

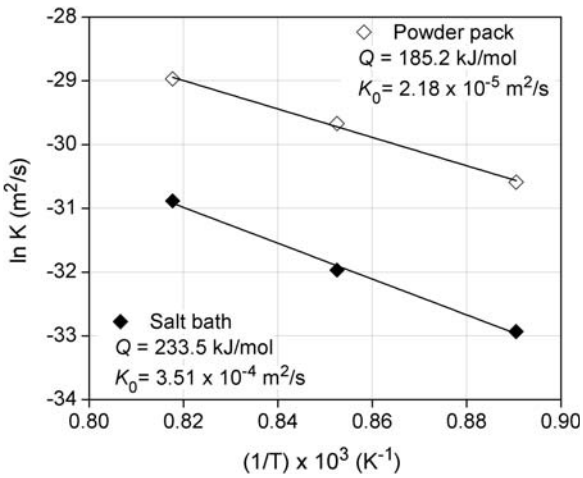

Fig. 5. Growth rate constant versus reciprocal boronizing temperature of the martensitic stainless steel AISI 420 specimens boronized using salt bath and powder pack.

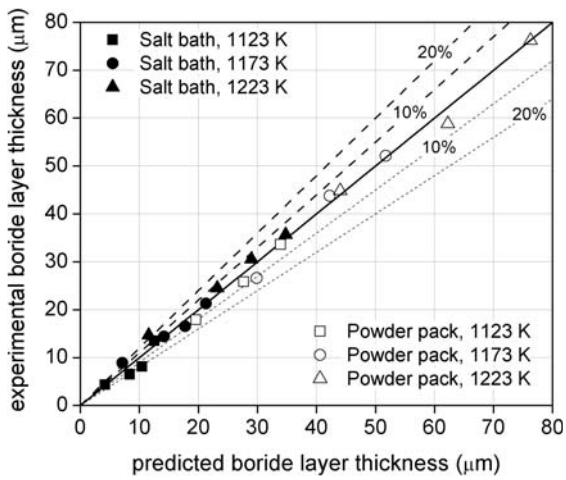

Fig. 6. All experimental boride layer thicknesses versus all predicted boride layer thicknesses.

ation energies and empirical data, K_0, are summarized in Table 1. The activation energy of boronizing process using commercial powder pack is 185.2 kJ mol^{-1}. This value seems lower than that of other martensitic stainless steel AISI 440C as reported in [11]. It should be due to higher carbon and chromium contents in the martensitic stainless steel AISI 440C. Accordingly, the boride layer thicknesses on martensitic stainless steel AISI 420 are higher than those of the martensitic stainless steel AISI 440C. From Table 1, the activation energy of the boronizing process using commercial powder pack is also lower than that of the boronizing process using molten borax with added Fe-Si 15 wt.% (233.5 kJ mol^{-1}). Thus, higher boride layer thicknesses of the packed boronizing process were detected as illustrated in Figs. 1a,b.

From a combination of Eq. (1) and Eq. (2), the prediction of boride layer thickness as a function of boronizing temperature and time, which is very important and useful particularly from the perspective of the manufacturers, is expressed in Eq. (3):

$$d = 10^6 \times \sqrt{K_0} \sqrt{t \exp\left(-Q/RT\right)}. \qquad (3)$$

Finally, the prediction formula of the boride layer thickness (in μm) can be finally established and summarized in Table 1. In addition to the coefficient of correlation (R^2) of each correlation and the mean absolute percentage error, MAPE in Eq. (4) have been calculated to show about their accuracies as follows:

$$\text{MAPE} = \frac{1}{n} \sum_{i=1}^{n} \left| \frac{E_i - P_i}{E_i} \right| \times 100, \qquad (4)$$

where E is the data from experiments, P is the data from the prediction formulas in Eq. (3). The coefficient of correlation (R^2) of each correlation and the mean absolute percentage error are shown also in Table 1. To demonstrate accuracies, all experimental data were compared to the predicted data in one diagram as shown in Fig. 6. The predicted data were calculated using the boronizing parameters, Q and K_0, from the experiments in Table 1. Considering results of analysis listed in Table 1 and Fig. 6, it is possible to mention that the prediction with respect to industrial application should be acceptable. Finally, simulation diagrams of boride layer thicknesses on the martensitic stainless steel AISI 420 using the molten borax and

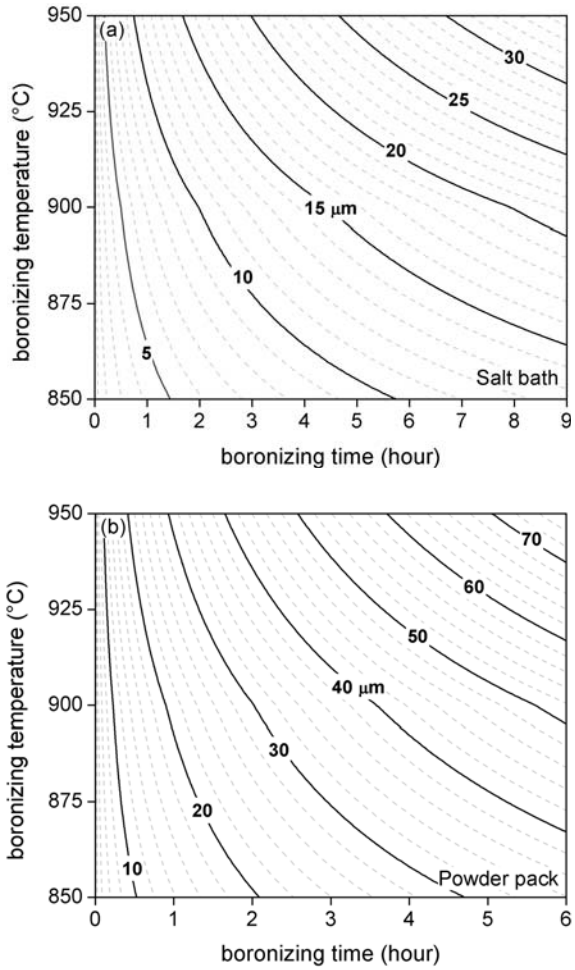

Fig. 7. Simulated boride thicknesses as a function of boronizing temperature and time for using (a) salt bath and (b) powder pack.

the commercial pack powder are established and depicted in Figs. 7a,b.

4. Conclusions

The formed boride layers on the martensitic stainless steel AISI 420 using the molten borax with added Fe-Si 15 wt.% and commercial powder pack have relatively smooth and more compact morphology. Single phase Fe_2B was found, if the free boron atoms in the media are relatively low with the lower boronizing temperature and time. Boride layer thicknesses increase with increasing boronizing temperature and time taking into account the diffusion theory. Diffusion and Arrhenius equations can be used to describe kinetics of the boronizing process on the martensitic stainless steel AISI 420. Activation energies of 233.5 and 185.2 kJ mol^{-1} were determined for the borided martensitic stainless steel AISI 420 using the molten borax with added Fe-Si 15 wt.% and commercial powder pack, respectively. Simulation diagrams of boride layer thicknesses as a function of boronizing temperatures and times concerning industrial application could be acceptable.

Acknowledgements

The author would like to express sincere thanks to the National Metal and Materials Technology Center, Thailand, under grant no. MT-B-52-MET-11-210-G and the National Research Council of Thailand (NRCT) under grant no. 92.54 for financial support. Thanks are also due to Ms. R. Teerachavalkiat and Ms. L. Angkurarach for experimental works.

References

[1] Sinha, A. K.: ASM Handbook: Heat Treating. Materials Park, ASM International 1991.
[2] Davis, J. R.: Surface Hardening of Steels: Understanding the Basics. Materials Park, ASM International 2002.
[3] Selcuk, B., Ipek, R., Karamis, M. B.: J Mater Process Tech, *141*, 2003, p. 189. doi:10.1016/S0924-0136(02)01038-5
[4] Martini, C., Palombarini, G., Poli, G., Prandstraller, D.: Wear, *256*, 2004, p. 608. doi:10.1016/j.wear.2003.10.003
[5] Er, U., Par, B.: Wear, *261*, 2006, p. 251. doi:10.1016/j.wear.2005.10.003
[6] Kariofillis, G. K., Kiourtsidis, G. E., Tsipas, D. N.: Surf Coat Tech, *201*, 2006, p. 19. doi:10.1016/j.surfcoat.2005.10.025
[7] Campos, I., Palomar, M., Amador, A., Ganem, R., Martinez, J.: Surf Coat Tech, *201*, 2006, p. 2438. doi:10.1016/j.surfcoat.2006.04.017
[8] Kayali, Y., Anaturk, B.: Mater Design, *46*, 2013, p. 776. doi:10.1016/j.matdes.2012.11.040
[9] Taktak, S.: Surf Coat Tech, *201*, 2006, p. 2230. doi:10.1016/j.surfcoat.2006.03.032
[10] Sen, S., Sen, U., Bindal, C.: Mater Lett, *60*, 2006, p. 3481. doi:10.1016/j.matlet.2006.03.036
[11] Kayali, Y., Gunes, I., Ulu, S.: Vacuum, *86*, 2012, p. 1428. doi:10.1016/j.vacuum.2012.03.030
[12] Ozbek, I., Bindal, C.: Vacuum, *86*, 2011, p. 391. doi:10.1016/j.vacuum.2011.08.004
[13] Ozdemir, O., Omar, M. A., Usta, M., Zeytin, S., Bindal, C., Ucisik, A. H.: Vacuum, *83*, 2008, p. 175. doi:10.1016/j.vacuum.2008.03.026
[14] Efe, G. C., Ipek, M., Ozbek, I., Bindal, C.: Mater Charact, *59*, 2008, p. 23. doi:10.1016/j.matchar.2006.10.007
[15] Genel, K.: Vacuum, *80*, 2006, p. 451. doi:10.1016/j.vacuum.2005.07.013
[16] Sen, S., Sen, U., Bindal, C.: Surf Coat Tech, *191*, 2005, p. 274. doi:10.1016/j.surfcoat.2004.03.040
[17] Keddam, M.: Appl Surf Sci, *257*, 2011, p. 2004. doi:10.1016/j.apsusc.2010.09.043

[18] Uslu, I., Comert, H., Ipek, M., Celebi, F. G., Ozdemir, O., Bindal, C.: Mater Design, *28*, 2007, p. 1819. doi:10.1016/j.matdes.2006.04.019

[19] Genel, K., Ozbek, I., Bindal, C.: Mat Sci Eng A, *347*, 2003, p. 311. doi:10.1016/S0921-5093(02)00607-X